A response surface methodology to address uncertainties in cap rock failure assessment for CO2 geological storage in deep aquifers

Jeremy Rohmer, Olivier Bouc

A response surface methodology to address uncertainties in cap rock failure assessment for CO_2 geological storage in deep aquifers

Jeremy Rohmer[1], Olivier Bouc

BRGM, France

[1]Corresponding author at:

BRGM, 3 av. C. Guillemin BP36009, F-45060 Orléans Cedex 2, France.

Tel.: (+33) 2 38 64 30 92; fax: (+33) 2 38 64 36 89.

E-mail address: j.rohmer@brgm.fr

Abstract:

Cap rock failure assessment, either tensile fracturing or shear slip reactivation of pre-existing fault, is a key issue for preventing CO_2 leakage from deep aquifer reservoirs up to the surface. For an appropriate use in risk management, the uncertainties associated with such studies should be investigated. Nevertheless, uncertainty analysis requires

[1] Corresponding author at. BRGM, 3 av. C. Guillemin BP36009, 45060 Orléans Cedex 2, France.
Tel.: +33 2 38 64 30 92; fax: +33 2 38 64 36 89.
E-mail address: j.rohmer@brgm.fr

multiple simulations and a direct use of conventional numerical approaches might be too computer time-consuming. An alternative is to use conventional analytical models, but their assumptions appear to be too conservative. An intermediate approach is then proposed based on the response surface methodology, consisting in estimating the effective stress state after CO_2 injection as a linear combination of the most influential site properties based on a limited number of numerical simulations. The decision maker is provided with three levels of information: (1) the identification of the most important site properties; (2) an analytical model for a quick assessment of the maximal sustainable overpressure and (3) a simplified model to be used in a computationally intensive uncertainty analysis framework. This generic methodology is illustrated with the Paris basin case using a large scale hydromechanical model to assess caprock failure in the injector zone.

Keywords: CO_2 geological storage; Tensile fracturing; Shear failure; Response surface method; Sensitivity analysis; Uncertainty analysis

Nomenclature

b	Biot's coefficient
c'	Coefficient of internal cohesion (Pa)
$d\sigma_v$	Lithostatic vertical total stress gradient (Pa/m)
E	Young's modulus (Pa)
f	Numerical model
F_s	Shear slip failure criterion

F_t	Tensile failure criterion
g	Response surface model
H	Layer thickness (m)
k	Intrinsic permeability (m^2)
K_0	Initial stress state (defined as σ_h/σ_v)
nX	Number of input variables
N_S	Number of samples
P	Pore pressure (Pa)
P_{inj}	Injection pressure (Pa)
P_{cs}	Maximal sustainable overpressure, shear failure (Pa)
P_{ct}	Maximal sustainable overpressure, tensile failure (Pa)
R^2	Coefficient of determination
$RMSE$	Root mean square error
R_T	Tensile strength (Pa)
X	Vector of model input variables
X^*	Vector of most influential input variables
x	Model input variable
z_{inj}	Injection depth (m)

Greek symbols

β	Linear regression coefficient
$\Delta P.$	Pore pressure change (Pa)
δ_{ij}	Kronecker symbol = 0 if i ≠ j, =1 otherwise
φ'	Angle of internal friction (°)

μ	Mean of the training data
σ	Total stress (Pa)
σ'_v	Vertical effective stress (Pa)
σ'_h	Horizontal effective stress (Pa)
σ'_m	Mean effective stress (Pa)
τ	Maximal shear stress (Pa)
υ	Poisson's ratio
ω	Porosity (%)

1 Introduction

CO_2 capture and geological storage (denoted CCS) is seen as a promising technology in the portfolio of measures required to mitigate the effects of anthropogenic greenhouse gas emissions (IPCC, 2005). Among the available options, geological storage in deep aquifers is recognized to offer very large potential storage capacity with a broad distribution throughout the world in all sedimentary basins (e.g. Bachu, 2002). A prerequisite to its large-scale implementation is demonstrating its safety.

Among others, ensuring cap rock integrity constitutes one of the key aspects of safety. Deep aquifers are open geological systems, which commonly lack structural confinement; caprock layers represent sealing and confining geological units for such CO_2 geological storage sites. Several authors (Streit and Hillis, 2004; Hawkes et al., 2005; Rutqvist et al., 2007 and 2008; Vidal-Gilbert et al., 2008) have shown that CO_2 injection operations lead to reservoir fluid pressure increase and to mechanical stresses changes, which might potentially induce creation of new fractures or reactivation of pre-

existing faults in the caprock layers. These mechanical discontinuities (fault or fracture) represent leakage pathways (e.g. Wiprut and Zoback, 2000) for CO_2 to escape from the deep aquifer reservoir, hence generating potential risks for the humans and the environment (Holloway, 1997), and also decreasing, if not ruining, the efficiency of the storage to mitigate climate change. Other damaging effects might be associated with fracturing or fault reactivation such as ground surface subsidence (e.g. Feignier and Grasso, 1990) or in extreme cases, induced earthquakes (e.g. Sminchak and Gupta, 2003).

From a practical point of view, caprock failure assessment is carried out using predictive models that involve a large number of parameters. Uncertainty is an unavoidable aspect owing to the limited knowledge of the complex underground system, no matter how extensive site characterisation may be. A proper caprock failure assessment should include management of the sources of uncertainty associated with the underground medium, as outlined for instance in the proposal for European Directive on CO_2 geological storage (EC, 2008, Annex I, 3.3.4 "Risk characterisation"). For an appropriate use in CCS risk management, uncertainty analysis should be flexible regarding the nature of the available data, easily adaptable to the enrichment of storage site knowledge and its computation should be time-efficient. A large number of approaches exist to carry out uncertainty analysis, such as Monte Carlo sampling methods in a probabilistic framework (Fishman, 1996), Fuzzy sets (Zadeh, 1965), "hybrid" methods using fuzzy sets and probability distributions (e.g. Guyonnet et al., 2003). These approaches either rely on optimization or on random based procedures, hence requiring multiple model simulations, which may be computationally intensive when applied to a high-fidelity simulation code used for caprock failure assessment. To

meet such constraints, replacing the complex models by a simplified analytical model appears to be a good solution, as it can be easily and rapidly computed. Furthermore, such simplified models can be used in methodological frameworks to help regulating authorities and stakeholders auditing risk assessment procedures (for instance, Bouc et al., 2008; Oldenburg et al., 2009).

In this context, the objective of the current work is to develop simplified models to carry out uncertainty analysis in caprock failure assessment in a view to inform risk management. The first part of the paper gives an overview of the conventional approaches (both numerical and analytical) to address caprock failure tendency. The limitations of both approaches are outlined regarding two requirements: (1) the multiple model simulations of the uncertainty analysis; (2) the simplicity, practicability and flexibility of the risk models to guide risk management. In a second part, an alternative strategy is described based on the response surface methodology (Box and Draper, 1987). Such a methodology has already been successfully used in other fields such as structural reliability problems (Bucher and Bourgund, 1990), radioactive waste disposal (Helton, 1993), environmental aspects (Iooss et al., 2006). A third part illustrates the use of the simplified models to guide decision making for geomechanical risk management in the context of the French Paris Basin, based on the studies carried out in the PICOREF project (Brosse et al., 2006; Grataloup et al., 2008).

2 Caprock failure tendency assessment

Various studies, either at theoretical or at experimental level, have shown that rock mechanical failure is controlled by the effective stress σ', which can be defined as follows (Terzaghi, 1943).

$$\sigma'_{ij} = \sigma_{ij} - P\delta_{ij} \quad (1)$$

Where δ is the Kronecker symbol (δ_{ij}=0 if i≠j and δ_{ij}=1 otherwise) and σ is the total stress.

Several authors (Streit and Hillis, 2004; Hawkes et al., 2005; Rutqvist et al., 2007 and 2008; Vidal-Gilbert et al., 2008) have shown that the CO_2-injection operations lead to an increase in the pore pressure inside and around the host reservoir, which results in a general decrease of the effective stress (by convention, compressive stress is positive). Two main mechanical failure mechanisms have to be taken into account when predicting the performance of a particular site for CO_2 sequestration (e.g. Rutqvist et al., 2007 and 2008), namely: (1) tensile fracturing and (2) Shear slip reactivation of pre-existing fractures and faults.

2.1 *Tensile fracturing*

A tensile fracture can be induced provided that the minimal effective stress σ'_3 becomes negative (by convention, compressive stress is positive) and its absolute magnitude exceeds the tensile strength either of the rock matrix or of the fracture (denoted R_T). In an objective of risk management, we consider that the most critical tensile fracture is vertical, as it represents a direct conduit from the host reservoir to the surface. In the present study, the tensile failure criterion F_t is defined such that $\sigma'_3=\sigma'_h$ as follows:

$$F_t(R_T, \sigma'_h) = -(R_T + \sigma'_h) \quad (2)$$

Tensile fracturing appears provided that $F_t \geq 0$.

2.2 *Shear slip fault reactivation*

The potential for shear slip along pre-existing faults (or fractures) can be defined based on the Coulomb criterion, using the maximum shear stress τ, which acts along the fault plane, and on the mean effective stress σ'_m (Jaeger and Cook, 1969). In an objective of risk management, we assume that a cohesionless fault could exist at any point of the studied zone with an arbitrary orientation following the methodology described in (Rutqvist et al., 2007 and 2008). The Coulomb criterion can be written in the principal stress plane (Jaeger and Cook, 1969) as follows:

$$\left|\tau\right| = \sigma'_m \sin(\varphi') + c'\cos(\varphi') \quad (3)$$

Where c' is the fault coefficient of internal cohesion and φ' is the fault angle of internal friction. φ' depends on the fault static coefficient of friction, whose lower-limit value is 0.6 based on field observations in fractured rock masses. This corresponds to φ'=30° (e.g. Streit and Hillis, 2004). Nevertheless, caprock layers are usually shale geological formations (e.g. Birkholzer et al., 2009) and faults may contain clay minerals such that φ' may be lower than 30° (Byerlee, 1978). Thus, shear slip failure analysis is conducted considering a conservative lower bound of 15° (least likely value) and a plausible upper bound of 30° (most likely value).

The shear and mean stress components can be written using the effective principal stress components (σ'_1 ; σ'_3) such that:

$$\left|\tau\right| = 0.5(\sigma'_1 - \sigma'_3) \quad (4)$$

$$\sigma'_m = 0.5(\sigma'_1 + \sigma'_3) \quad (5)$$

In the present study, we consider that the most critical faults are cohesionless (i.e. c'=0) with a "sub-vertical" orientation. In such a case, the shear slip failure criterion F_s is defined such that $\sigma'_3=\sigma'_h$ and $\sigma'_1=\sigma'_v$ as follows:

$$F_s(\varphi', \sigma'_h, \sigma'_v) = (\sigma'_v - \sigma'_h) - (\sigma'_v + \sigma'_h)\sin(\varphi') \quad (6)$$

A "sub vertical" pre-existing cohesionless fault is reactivated provided that $F_s \geq 0$.

2.3 *Numerical analysis*

The effective stress state after injection can be investigated by means of numerical computer code. A commonly used technique is the finite element method (see Jing and Hudson, 2002 for an overview). This technique can take into account, among others, complex geological architectures, complex injection scenarios, coupling between different physical phenomena and various types of rock materials.

Hereafter, we describe a typical numerical large scale coupled hydraulical and geomechanical model to assess caprock failure tendency in the injector zone of a multilayered geological system such as the French Paris basin case.

2.3.1 Geometry and boundary conditions

Fig. 1 represents the geometry and the boundary conditions of the numerical model. The model is axisymmetric so that the injector well represents the vertical axis of symmetry

(left boundary). The multilayered system consists of the deep aquifer reservoir (denoted in abbreviated form *RES*), the caprock (denoted *CAP*), the basement (denoted *BAS*) and the overburden (denoted *OVE*) formation. A large lateral extent (100 km) is chosen so that the boundary condition has minimal effect on the simulation results. At this distance, the initial hydrostatic pressure is imposed. Vertical displacement at the bottom and horizontal displacement at the lateral boundaries are fixed.

[Fig. 1 about here]

2.3.2 **Modelling assumptions**

The problem is solved in the framework of the isothermal saturated porous media using the fully coupled hydromechanical simulator Code_Aster (e.g. Chavant et al., 2002). The mechanical behaviour of the rock matrix is elastic and governed by the Young's modulus (denoted E) and the Poisson's ratio (denoted υ). Hydraulical properties are defined by the intrinsic permeability (denoted k) and the porosity (denoted ω).

The initial pore pressure is hydrostatic. The initial stress state is determined by the ratio K_0 between the vertical and the horizontal total stress components and the lithostatic vertical total stress gradient $d\sigma_v$.

The porous medium is fully saturated by a unique fluid so that CO_2 injection is modelled by a gradual increase of the pore pressure. The pressure load P_{inj} is imposed along the thickness of the reservoir layer (left boundary, see Fig. 1) and the effective stress state evolution is assessed in the injector zone at the interface between the caprock and the reservoir layer after one year of injection. This zone is viewed as the

most critical zone, because injection-induced pressure buildup is maximal there, as shown by Birkholzer et al. (2009).

The proposed numerical model only remains valid for an analysis of the effective stress state evolution within the injector zone. Outside this zone, a more complex model should be used, such as a sequential coupling between a multiphase and multicomponent fluid flow transport code (to describe the behaviour of the supercritical CO_2 in the saline aquifer) and a mechanical code (Rutqvist et al., 2007 and 2008, Vidal-Gilbert et al., 2008). The use of such models is beyond the scope of the present paper and represents a perspective for further works. Note that the uncertainty methodology proposed in this paper is generic and can be applied to such models as well.

2.3.3 **Limitations for uncertainty analysis**

The model mesh consists of more than 24000 nodes and almost 50000 elements with a minimal mesh dimension of 50 cm in the injector zone. The computer time for a single simulation ranges from 10 to 30 minutes with an average value of 15 minutes depending on the input variables. Uncertainty analysis implies exhaustive simulations of multiple stochastic realizations. The number of simulations can be very large depending on the number of uncertainty sources and above all, when the objective is to assess the occurrence of very low probability events. Thus, conducting such an analysis using the described numerical model appears to be too computationally intensive and thereby too time consuming.

2.4 *Conventional analytical methods*

A good alternative is to replace the large scale complex numerical model by a simplified analytical model. Two commonly used analytical methods are described as follows (e.g. Rutqvist et al., 2007).

2.4.1 **Analytical approach n°1**

We assume that pressure distribution is homogeneous in the aquifer layer and that the in situ stress field remains unchanged during injection. In this case, the total stress state after injection remains constant to the remote total stress state so that changes in the effective stresses (either horizontal or vertical) exactly correspond to the opposite of the changes in the pore pressure ΔP.

2.4.2 **Analytical approach n°2**

A second approach consists in assuming a simplification of the reservoir geometry (e.g. Streit and Hillis, 2004; Hawkes et al., 2005). The aquifer layer can be modelled by an idealized thin and laterally extensive reservoir. In this case, the vertical total stress is assumed equal to the remote total stress, whereas the horizontal total stress depends on the Poisson's ratio υ, on the Biot's coefficient b, and on the pore pressure change ΔP (i.e. the so-called "poroelastic effect").

$$\Delta\sigma_3 = b\frac{(1-2\upsilon)}{1-\upsilon}\Delta P \qquad (7)$$

2.4.3 **Limitations for uncertainty analysis**

Rutqvist et al. (2007) have shown that the described analytical approaches might lead either to an over- or to an under- estimation of the maximal sustainable injection

pressure. An additional comparison study is carried out in this section. The tensile failure criterion (with R_T=0) and the shear slip failure criterion of a cohesionless fault (with φ'=30°) are evaluated at the interface of the caprock and the reservoir layer in the injector zone at z_{inj}=1500 m. We use the previously described numerical model and both analytical models. Several randomly generated material and site configurations are defined based on the assumptions in Table 1.

[Fig. 2 about here]

Fig. 2 depicts the comparison between the numerically and analytically estimated failure criteria. The straight black line represents the first bisector. The closer the dots to the straight line, the better the agreement between the numerical and the analytical analysis. It appears that the tensile failure criterion is overestimated by both conventional analytical approaches, whereas the shear slip failure criterion is overestimated for the highest values and underestimated for the lowest values. The assumptions on which conventional analytical models are based appear to be too conservative. This result is consistent with Rutqvist et al. (2007), who concluded that numerical analysis results in a more accurate estimation of the maximum sustainable CO_2 injection pressure, because it can assess the injection-induced spatial evolution of both fluid pressure and stress, including important mechanical interactions between the reservoir and the caprock layer.

Other analytical models exist. The most recent model is developed by Soltanzadeh and Hawkes (2008) with application in (Soltanzadeh and Hawkes, 2009) based on the Eshelby's theory of inclusions for a poroelastic material. Nevertheless, such model

shows limitations regarding the objective of the paper, as it cannot account for multilayered cases where mechanical properties of the reservoir are different from those of the surrounding rock, as outlined by Soltanzadeh and Hawkes (2008). Besides, it appears to be more adapted for reservoir of finite extension such as oil and gas reservoirs.

3 Response surface strategy

The assumptions, on which conventional analytical approaches are based, appear too constraining for uncertainty analysis. Numerical approaches may entail a heavy computational burden for uncertainty analysis. An intermediate solution between both approaches is proposed in the framework of the response surface methodology (Box and Draper, 1987) to take advantage of the accurate estimation of the numerical analysis and of the low computational cost of analytical analysis.

3.1 *Objective*

The objective is to develop analytical models using the previously described numerical model to estimate the horizontal and vertical effective stresses (σ'_h ; σ'_v) at the interface between the caprock and the reservoir layer. To limit computer time cost, only a finite number of numerical simulations are run (step 1 of the response surface methodology). A catalogue of analytical models is constructed for different combinations ($d\sigma_v$; z_{inj}) of lithostatic vertical total stress gradients and of injection depths, which are viewed as design parameters for the storage site. The main difficulty stems from the number of input variables of the numerical model (in total 20). A sensitivity analysis is carried out to select the most influential variables of the numerical model (step 2). The

approximation quality of (σ'_h ; σ'_v) is then assessed (step 3) in the view to use such models for uncertainty assessment.

3.2 *Response surface method*

Formally, let us consider the numerical model *f* defined as follows:

$$\sigma' = f(X) = f(x_1, x_2, ..., x_{nX}) \quad (8)$$

Where $X=[x_1,...,x_{nX}]$ corresponds to the vector of the *nX* input variables of the numerical models. We consider in total 20 input variables (see Table 1). σ' represents the numerically calculated effective stress (either horizontal or vertical) in the injector zone at the interface between the caprock and the reservoir layer.

The response surface method (Box and Draper, 1987) consists in constructing a function that simulates the behaviour of the real model in the space of the input variables. The complex numerical model *f* is replaced by a mathematical approximation *g*, referred to as a response surface model. In this study, a first order polynomial (i.e. a linear regression model) is used as in Equation (9).

$$\sigma' = f(X) \approx g(X) = \beta_0 + \sum_{j=1}^{nX} \beta_j x_j \quad (9)$$

The objective is to determine the *nX* regression coefficients β using a least squares regression analysis.

3.3 *Step 1: generation of the training data*

The linear regression is based on a mapping of observation samples of the form $\{X^j, \sigma^j\}$ (with j ranging from 1 to the total number of pairs N_S). The mapping is referred to as the training data of the response surface. The samples are generated randomly through the Latin hypercube sampling method (McKay et al., 1979 and further developed by Iman et al., 1981). This sampling method is combined with the "maxi min" space filling design criterion (Koehler and Owen, 1996) to maximise the exploration of the input variable domain. A sample of N_S=100 simulations has been generated based on the assumptions in Table 1. Note that intrinsic permeabilities are expressed using the Darcy unit (denoted D): 1 D corresponds to 1.10^{-12} m².

[Table 1 about here]

Table 1 represents the validity domain of the developed model and is defined using typical properties of the aquifer formations for CO_2 geological storage, with high intrinsic permeability and porosity, and of caprock layers, such as shale formations, with low intrinsic permeability and porosity (e.g. Birkholzer et al., 2009 and Rutqvist et al., 2007 and 2008).

Note that $K_0 \leq 1.0$, so that the simplified models are developed for an extensional stress regime. In such a stress regime, Soltanzadeh and Hawkes (2009) have demonstrated that only faults located in rocks overlying and underlying the reservoir tend towards reactivation, which is seen as the most critical event for the mechanical integrity of storage reservoir. In a compressional stress regime (i.e. $K_0 \geq 1.0$), fault reactivation is more likely to occur within the reservoir and adjacent to its flanks.

3.4 *Step 2: most sensitive variable selection*

The numerical model presents a large number of input variables (in total 20). Each input variable has a different influence on the numerical model outputs. A sensitivity analysis is conducted to identify the contributions of individual inputs to the uncertainty in analysis outcomes to keep only the most influential parameters in the response surface model (Saltelli et al., 2000). In this view, a forward stepwise selection procedure is chosen (e.g. Storlie and Helton, 2008). It operates in the following manner.

In a first step, a response surface model is constructed for each candidate input variable using Equation (9). This results in *nX* one-dimensional linear models. The best of these models is identified using the root mean square error *RMSE*, which is defined as follows:

$$RMSE = \frac{1}{N_S}\sqrt{\sum_{j=1}^{j=Ns}(g(X^j) - f(X^j))^2} \quad (10)$$

The one-dimensional model with the minimal *RMSE* is selected and the corresponding input variable, say for instance x_1, is identified as the most important input variable. In a second step, two-dimensional response surface models are constructed using the best candidate x_1, selected in the first step and each of the remaining nX–1 input variables. The parameter, say for instance x_2, associated with the minimal *RMSE* is selected. In a third step, three-dimensional response surface models are constructed using the best candidates x_1 and x_2, respectably selected in the first and second step, and each of the remaining nX–2 input variables. Following the same principle, the third best candidate is selected and the process is continued until the selection criterion *RMSE* has reached an "acceptable" threshold.

[Fig. 3 about here]

Fig. 3 depicts the variable selection respectably for (σ'_h ; σ'_v) for $d\sigma_v$=0.0245 MPa/m and z_{inj}=1500 m. After selection of the first variable, the *RMSE* of the best response surface models for (σ'_h ; σ'_v) respectably reaches 3.40 MPa and 1.06 MPa. These values remain too large regarding the objective of uncertainty analysis and the selection procedure is continued. The *RMSE* decreases to reach respectably 1.06 MPa and 0.67 MPa during the second step of the selection procedure. The selection procedure is repeated six times until the *RMSE* reaches less than 3.5 bars for both stress components. This threshold represents less than 3 % of the mean of the training data for both stress components. This can be considered an "acceptable" threshold. Besides, an additional selection step does not provide any significant decrease of *RMSE* and the selection procedure is then stopped.

3.5 *Step 3: validation procedure*

To use the response surface models as predictive models in the framework of an uncertainty analysis, the quality of the approximation should be assessed. We propose a cross-validation approach, which consists in estimating how well the response surface constructed from a set of training data is going to perform on future "as-yet-unseen" data. In this study, a "leave-one-out cross-validation" (e.g. Hjorth, 1994) approach is chosen. This technique involves using a single observation from the initial training data as the validation data, and the remaining samples as the new training data. A linear regression is performed with the new training data in order to predict the validation data. This procedure is repeated so that each observation in the initial training data is

used once as a validation data. Fig. 4 depicts the numerically calculated effective stress (horizontal and vertical) versus the estimated effective stress using the response surface model for $d\sigma_v$=0.0245 MPa/m and z_{inj}=1500 m.

[Fig. 4 about here]

The estimated data are close to the straight black line (first bisector), hence indicating a good approximation. A metric of the approximation quality is defined using the coefficient of determination (denoted R^2) as follows:

$$R^2 = \sum_{j=1}^{Ns-1} \left(\sigma'^{j}_{e} - \mu\right)^2 \Big/ \sum_{j=1}^{Ns} \left(\sigma'^{j} - \mu\right)^2 \quad (11)$$

Where σ' is the true value, σ'_e is the estimated value and μ the mean value of the training data. When the variation between the true and the estimated value is small, R^2 is close to 100 %, which indicates that the response surface model is successful in matching the observed results. In the case of Fig. 4, R^2 respectably reaches 99.0 % and 99.5 % for σ'_h and σ'_v.

4 Use for an informed decision, Paris Basin illustrative case

4.1 *Methodology*

The validated response surface models associated with (σ'_h ; σ'_v) are then used to estimate the cap rock failure criterion for the tensile mechanism F_t (Equation 2) and for the shear slip mechanism F_s (Equation 3) as a linear combination of the most important

site properties X^* and of the injection pressure P_{inj}. Let us define the overpressure as the difference between the injection pressure and the initial pore pressure. The maximal sustainable overpressure P_{ct} and P_{cs} for both failure mechanisms can then be expressed, such that $F_t(P_{ct} ; X^*)=0$ and $F_s(P_{cs} ; X^*)=0$ as a linear combination of the selected site properties X^*. Such linear models provide three levels of information for an efficient support decision making in CCS risk management. The French Paris basin is used as an illustration case, for which $d\sigma_v$ reaches 0.0245 MPa/m and z_{inj} reaches 1500 m (Vidal-Gilbert et al., 2008).

4.2 *Level 1: prioritisation and sensitivity measure of site properties*

Knowledge increases with additional information and data, but for efficient risk management, it is important to know what source of information is critical and by how much its knowledge is useful. In other words, the site properties on which the effort should be made to have sufficient knowledge should be prioritised. In this view, the response surface model provides the selection of the most influential site properties (step 2 of the response surface methodology).

Furthermore, the linear regression coefficients associated with P_{ct} and P_{cs} directly measure the sensitivity of each site property. Note that the input variables are normalised between 0 and 1. When the regression coefficient is positive, the relationship is direct so that the critical injection pressure increases, if the site property increases. When the regression coefficient is negative, the tendency is inverted.

[Fig. 5 about here]

Fig. 5 depicts the regression coefficients for both maximal sustainable overpressures P_{ct}

(with tensile strength R_T=0) and P_{cs} (for a cohesionless pre-existing fault with φ'=30°). This analysis shows that the most sensitive site property is the initial stress state K_0. The relationship is direct so that storage sites with the lowest initial stress state present the highest risk of caprock failure and injection pressure in such storage sites should be carefully controlled. This result is consistent with the conclusions of Hawkes et al. (2005) and of Rutqvist et al. (2007 and 2008). The Poisson's ratios υ_{CAP} and υ_{RES} are selected as second and third sources of uncertainty so that storage sites with the highest Poisson's ratio present the highest risk of caprock failure.

Based on this analysis, the most critical configuration can be defined for all site properties (Table 2) so that the maximal sustainable overpressure P_{ct} and P_{cs} are minimized (considering the validity domain defined in Table 1).

[Table 2 about here]

4.3 *Level 2: conservative assessment of maximal sustainable overpressure*

Using the linear models of the failure criteria F_t and F_s, abacuses can be constructed under the form "overpressure versus most influential site properties".

[Fig. 6 about here]

Fig. 6 depicts the abacus for the tensile failure mechanism. The green coloured surface represents the failure surface with R_T ranging from 0 to 1 MPa.

We describe how such an abacus should be read. Let us consider an operator, who aims at injecting CO_2 with an overpressure twice the initial pore pressure. Fig. 6 gives the minimal value of the initial stress state K_0 (of 0.54) to prevent the cap rock from fracturing (with R_T=0), considering that all other parameters (namely υ_{CAP}, υ_{RES}, k_{RES} and H_{CAP}) are taken in the most critical configuration (Table 2). In the same manner, the minimal value for the Poisson's ratio of the cap rock layer υ_{CAP} should reach at least 0.24 at the same overpressure level. The critical values for the other parameters should be read following the same principle so that the configuration is always chosen as the most critical one, hence implying that this evaluation remains a conservative estimate.

[Fig. 7 about here]

Fig. 7 depicts the abacus for the shear slip failure mechanism considering a cohesionless pre-existing fault. The blue coloured surface represents the failure surface with φ' ranging from 15 to 30°. Following the same principle as for tensile failure mechanism, let us consider an operator, who aims at injecting CO_2 with an overpressure twice the initial pore pressure. Fig. 7 gives the minimal value of the initial stress state K_0 (of 0.605) to prevent a cohesionless pre-existing fault (with φ'=30°) from being reactivated, considering that all other parameters (namely υ_{CAP}, υ_{RES}, k_{RES}, H_{CAP}, k_{CAP} E_{RES} and k_{BAS}) are taken in the most critical configuration (Table 2).

4.4 *Level 3: uncertainty analysis*

The third level of analysis consists of the uncertainty assessment. Several approaches exist and we focus on the commonly used Monte Carlo method in a probabilistic

framework. Let us define the following random variables: (1) the horizontal effective stress and (2) the critical angle of internal friction, for which the shear slip failure of a cohesionless pre-existing fault is activated.

The objective of the Monte Carlo technique is to simulate the probability distribution of both random variables, given the probability distribution assigned to the site properties, which are seen as input random variables. In this technique, the input distributions are "recreated" through sampling and the failure criteria are calculated for each stochastic realization of the site properties. A large number of samples may be required for the successful implementation of this technique depending on the number of uncertainty sources. This number can also be very large when the objective is to assess the occurrence of very low probability events.

For each site property, we specify a probability distribution. Table 3 summarizes the assumptions and the references on which they are based. The probability distributions are either known or assumed. For instance, the probability distribution assigned to the reservoir intrinsic permeability k_{RES} is empirical and based on the statistical analysis of the permeability measurements carried out in the Dogger geological unit for geothermal purposes (Rojas et al., 1989). When the mathematical representation of the probability distribution is not known, we assume a uniform distribution based on the "maximum entropy" approach (Gzyl, 1995). For instance, the probability distribution assigned to the initial stress state K_0 is assumed to be uniform so that the lower and upper bounds are defined based on the studies of Cornet and Burlet (1992) and of Vidal-Gilbert et al. (2008). We use this methodology for all parameters with unknown probability distribution, except for the intrinsic permeability k_{CAP} and k_{BAS}, which are assumed to be log normal, based on the recent uncertainty analysis of Kovscek and Wang (2005).

[Table 3 about here]

We generate 1 million realizations of the site properties using the assumptions of Table 3. The average computer time for a single numerical code simulation reaches 15 minutes. If the uncertainty analysis had been directly computed with the computer code using 50 Central Processing Units, the total computer time would have reached more than 6 months. As the developed models are very simple (i.e. linear), they have a low computer time cost and can be quickly computed. The total computer time cost of the response surface model corresponds to the computation of 100 code simulations (training data) for the response surface construction (more than one day), to the cost of the validation procedure (more than one day), and to the cost to carry out the Monte Carlo technique using the response surface model (more than one day). Globally, it takes only between 3 and 4 days of computation.

[Fig. 8 about here]

Fig. 8 depicts the probability of exceeding a given threshold of horizontal effective stress at different overpressure levels. The analysis shows that the risk of creating vertical tensile fractures is very low for the considered assumptions in the context of the Paris basin case. The lowest tensile strength (R_T=0) is not reached even for the highest overpressure level (200 % of the initial overpressure).

[Fig. 9 about here]

Fig. 9 depicts the probability of exceeding a given threshold of angle of internal friction, for which the shear slip failure of a cohesionless pre-existing fault is activated. The analysis shows that the probability of exceeding a least likely value φ'=15° reaches 0.0188 % considering a low overpressure level (50 % of the initial pore pressure), 6.11 % considering a medium overpressure level (150 % of the initial pore pressure) and 62.22 % considering a high overpressure level (200 % of the initial pore pressure). The most likely threshold at φ'=30° is only reached with a probability of 15.15 % considering a high overpressure level.

5 Concluding remarks and further works

This paper presents a response surface methodology to develop simplified models to address uncertainties in cap rock failure assessment. The decision maker is provided with three main elements to be used for an informed CCS risk management: (1) the most sensitive site properties in the caprock failure analysis i.e. the parameters on which the characterisation effort should be made to have sufficient knowledge; (2) an analytical model of the effective stresses for a quick assessment of the maximal sustainable overpressure and (3) a simplified model to be used in a computationally intensive uncertainty analysis framework. The methodology has been illustrated with a large scale hydromechanical model to assess caprock failure in the injector zone of a multilayered geological system. In further works, such a generic approach can be applied to more complex models (for instance Rutqvist et al., 2007 and 2008, Vidal-Gilbert et al., 2008) to assess caprock failure and fault shear slip reactivation outside the injector zone. In the present study, the linear assumption for the response surface proves

to be appropriate, but further works should also be carried out using other regression techniques when facing complex non linear mathematical relationships (Storlie and Helton, 2008).

Acknowledgments

This work has been supported by French Research National Agency (ANR) through CO_2 program (project CRISCO2, n° ANR-06-CO2-003)

REFERENCES

Bachu, S., 2002. Sequestration of CO2 in geological media in response to climate change: road map for site selection using the transform of the geological space into CO2 phase space. Energy Convers. Manag. 43, 87-102.

Birkholzer, J.T., Zhou, Q., Tsang, C.-F., 2009. Large-scale impact of CO2 storage in deep saline aquifers: a sensitivity study on the pressure response in stratified systems. Int. J. of Greenhouse Gas Control 3, 181-194.

Bouc, O., Audigane, P., Bellenfant, G., Fabriol, H., Gastine, M., Rohmer, J., Seyedi, D., 2008. Determining safety criteria for CO2 geological storage. In: 9th International Conference on Greenhouse Gas Control Technologies, 16-20 November 2008, Washington, USA.

Box, G.E., Draper, N.R., 1987. Empirical model building and response surfaces, Wiley series in probability and mathematical statistics, John Wiley and Sons, New York, USA.

Brosse, E., de Smedt, G., Bonijoly, D., Garcia, D., Saysset, S., Manai, T., Thoraval, A., Crepin, S., 2006. PICOREF: towards an experimental site for CO2 geological storage in the ParisBasin, In: 8th International Conference on Greenhouse Gas

Control Technologies, 19-22 June 2006, Trondheim, Norway.

Bucher, C.G., Bourgund, U., 1990. Fast and efficient response surface approach for structural reliability problems. Structural Safety 7, 57-66.

Byerlee, J., 1978. Friction of rocks. Pure Appl. Geophys. 116, 615-626.

Chavant, C., Granet, S., Le Boulch, D., 2002. Modelling of a nuclear waste disposal: numerical and practical aspects, In: Thimus et al. (Eds), Biot conference on poromechanics II, Balkema, Rotterdam, 145-150.

Cornet, F.H., Burlet, D., 1992. Stress field determinations in France by hydraulic tests in boreholes. J. Geophys. Res. 97, 11829-11849.

EC (European Commission), 2008. Proposal for a Directive of the European Parliament and of the Council on the geological storage of carbon dioxide, COM (2008) 18 final, 23 January 2008, Brussels, Belgium. Available online at:
http://eur-lex.europa.eu/LexUriServ/LexUriServ.do?uri=COM:2008:0018:FIN:EN:PDF

Feignier, B., Grasso J.R., 1990. Seismicity induced by gas production. I. correlation of focal mechanisms and dome structure. Pure Appl. Geophys. 134, 405-426.

Fishman, G.S., 1996. Monte Carlo: Concepts, Algorithms and Applications, Springer Verlag, Berlin, Germany.

Guyonnet, D., Bourgine, B., Dubois, D., Fargier, H., Côme, B., Chiles, J.-P., 2003. Hybrid approach for addressing uncertainty in risk assessments. J. of Environmental Engineering 126, 68-78.

Grataloup, S., Bonijoly, D., Brosse, E., Garcia, D., Hasanov, V., Lescanne, M., Renoux, P., Rigollet, C., Thoraval, A., 2008. PICOREF: A site selection methodology for saline aquifer in Paris Basin. In: 9th International Conference on Greenhouse Gas Control Technologies, 16-20 November 2008, Washington, USA.

Gzyl, H., 1995. The Method of Maximum Entropy. In: Bellomo, F. Brezzi, N. (Eds.), Series on Advances in Mathematics for Applied Sciences, World Scientific Publishing Co, 29.

Hawkes, C.D., McLellan, P.J., Bachu, S., 2005. Geomechanical factors affecting geological storage of CO2 in depleted oil and gas reservoirs. J. Can. Pet. Technol. 44, 52-61.

Helton, J.C., 1993. Uncertainty and sensitivity analysis techniques for use in performance assessment for radioactive waste disposal. Reliability Engineering and System Safety 42, 327-367.

Holloway, S., 1997. Safety of the underground disposal of carbon dioxide. Energy Convers. Manag. 38, 241-245.

Hjorth, J.S.U., 1994. Computer Intensive Statistical Methods: Validation Model Selection and Bootstrap, Chapman and Hall, London, UK.

Iman, R.L., Helton, J.C., Campbell, J.E., 1981. An approach to sensitivity analysis of computer models, Part 1. Introduction, input variable selection and preliminary variable assessment. J. of Quality Technology 13, 174-183.

Iooss, B., Van Dorpe, F., Devictor, N., 2006. Response surfaces and sensitivity analyses for an environmental model of dose calculations. Reliability Engineering and System Safety 91, 1241-1251.

IPCC (Intergovernmental Panel on Climate Change), 2005. IPCC Special Report on Carbon Dioxide Capture and Storage. Cambridge University Press, New York, USA.

Jaeger, J.C., Cook, N.G.W., 1969. Fundamentals of rock mechanics, Methuen & Co. Ltd, London, UK.

Jing, L., Hudson, J.A., 2002. Civil Zone review paper, Numerical methods in rock mechanics. Int. J. of Rock Mechanics and Mining Sciences 39, 409-427.

Koehler, J.R., Owen, A.B., 1996. Computer experiment, In: Ghosh S. and Rao C.R. (Eds.), Handbook of Statistics. Elsevier Science, New York, USA, 13, pp. 261-308.

Kovscek, A.R., Wang, Y., 2005. Geologic storage of carbon dioxide and enhanced oil recovery. I. Uncertainty quantification employing a streamline based proxy for reservoir flow simulation. Energy Conv. Manag. 46, 1920-1940.

McKay, M.D., Beckman, R.J., Conover, W.J., 1979. A comparison of three methods for selecting values of input variables in the analysis of output from a computer code. Technometrics 21, 239-245.

Oldenburg, C.M., Bryant, S.L., Nicot, J.-P., 2009. Certification framework based on effective trapping for geologic carbon sequestration. Int. J. of Greenhouse Gas Control, (In Press), doi:10.1016/j.ijggc.2009.02.009

Rojas, J., Giot, D., Le Nindre, Y.M., Criaud, A., Fouillac, C., Brach, M., 1989. Caracterisation et modelisation du reservoir geothermique du Dogger, bassin parisien, France. Technical Report CCE, EN 3G-0046-F(CD), BRGM R 30 IRG SGN 89.

Rutqvist, J., Birkholzer, J.T., Cappa, F., Tsang, C.-F., 2007. Estimating maximum sustainable injection pressure during geological sequestration of CO2 using coupled fluid flow and geomechanical fault-slip analysis. Energy Convers. Manage. 48, 1798-1807.

Rutqvist, J., Birkholzer, J.T., Tsang, C.-F., 2008. Coupled Reservoir-Geomechanical Analysis of the Potential for Tensile and Shear Failure Associated with CO2

Injection in Multilayered Reservoir-Caprock Systems. Int. J. of Rock Mechanics and Mining Sciences 45, 132-143.

Saltelli, A., Chan, K., Scott, E.M., 2000. Sensitivity analysis, John Wiley and Sons, New York, USA.

Streit, J.E., Hillis, R.R., 2004. Estimating fault stability and sustainable fluid pressures for underground storage of CO2 in porous rock. Energy 29, 1445-1456.

Sminchak, J., Gupta, N., 2003. Aspects of induced seismic activity and deep-well sequestration of carbon dioxide. Environ. Geosci. 10, 81-89.

Soltanzadeh, H., Hawkes, C.D., 2008. Semi-analytical models for stress change and fault reactivation induced by reservoir production and injection. J. Pet. Sci. Eng. 60, 71-85.

Soltanzadeh, H., Hawkes, C.D., 2009. Assessing fault reactivation tendency within and surrounding porous reservoirs during fluid production or injection. Int. J. of Rock Mechanics and Mining Sciences 46, 1-7.

Storlie, C.B., Helton, J.C., 2008. Multiple predictor smoothing methods for sensitivity analysis: Description of techniques. Reliability Engineering and System Safety 93, 28-54.

Terzaghi, K., 1943. Theoretical Soil Mechanics, John Wiley and Sons, New York, USA.

Vidal-Gilbert, S., Nauroy, J-F., Brosse, E., 2008. 3D geomechanical modelling for CO2 geologic storage in the Dogger carbonates of the Paris Basin. Int. J. of Greenhouse Gas Control, (In Press), doi:10.1016/j.ijggc.2008.10.004

Wiprut, D., Zoback, M.D., 2000. Fault reactivation and fluid flow along a previously dormant normal fault in the northern North Sea. Geology 28, 595-598.

Zadeh, L.A., 1965. Fuzzy sets. Information and Control 8, 338-353.

LIST of FIGURES CAPTIONS

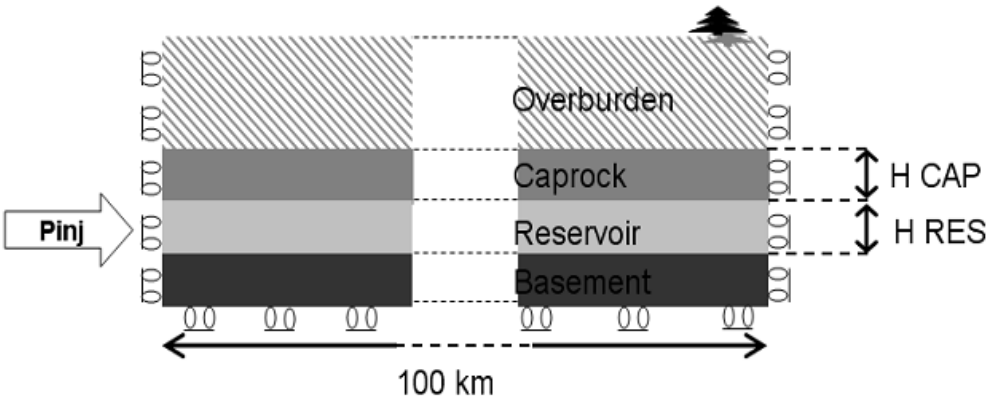

Fig. 1 - Geometry and boundary conditions of the large scale multilayered hydromechanical model.

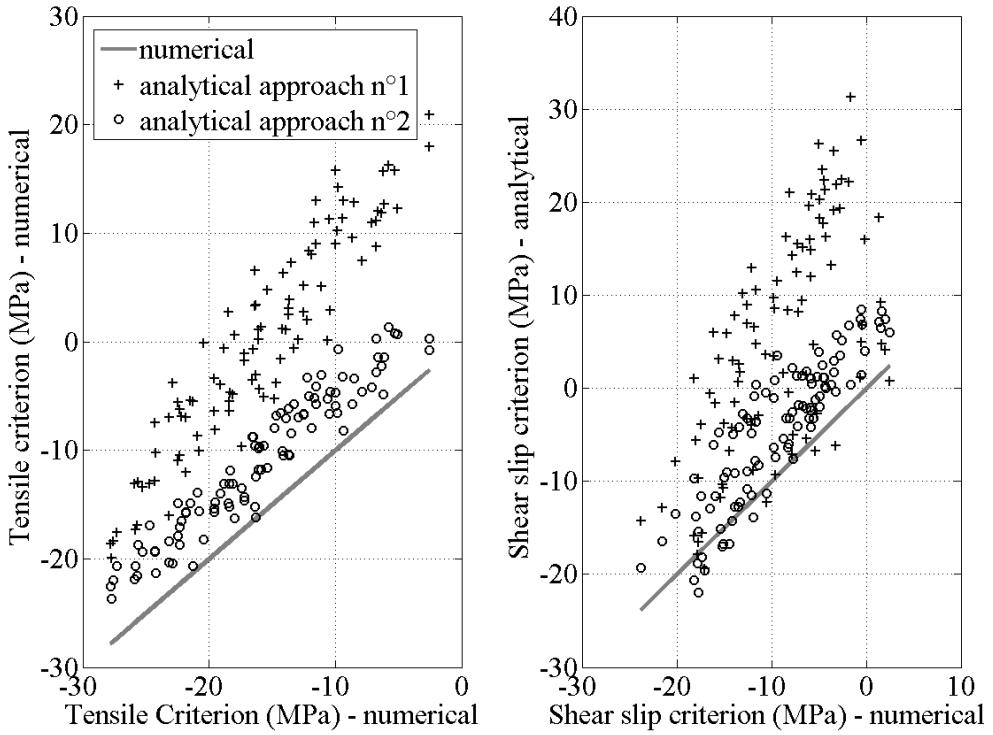

Fig. 2 - Comparison between the numerically and analytically estimated failure criteria, tensile mechanism with null tensile strength (left figure) and shear slip reactivation considering a cohesionless pre-existing fault with angle of internal friction of 30° (right figure).

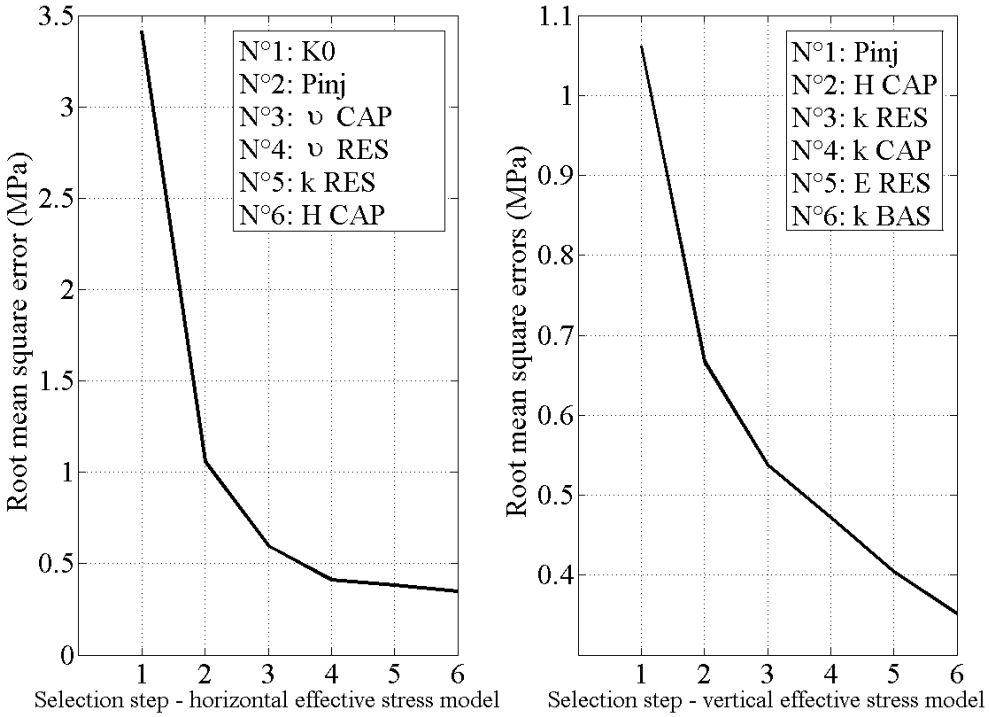
Root mean square error (MPa)
3.5
3
2.5
2
1.5
1
0.5
0
1
2
3
4
5
6
Selection step - horizontal effective stress model
N°1: K0
N°2: Pinj
N°3: υ CAP
N°4: υ RES
N°5: k RES
N°6: H CAP
Root mean square errors (MPa)
1.1
1
0.9
0.8
0.7
0.6
0.5
0.4
1
2
3
4
5
6
Selection step - vertical effective stress model
N°1: Pinj
N°2: H CAP
N°3: k RES
N°4: k CAP
N°5: E RES
N°6: k BAS

Fig. 3 - Evolution of the Root Mean Square Error during the selection procedure of the most influential input variables for the response surface model respectably associated with the horizontal (left figure) and the vertical (right figure) effective stress.

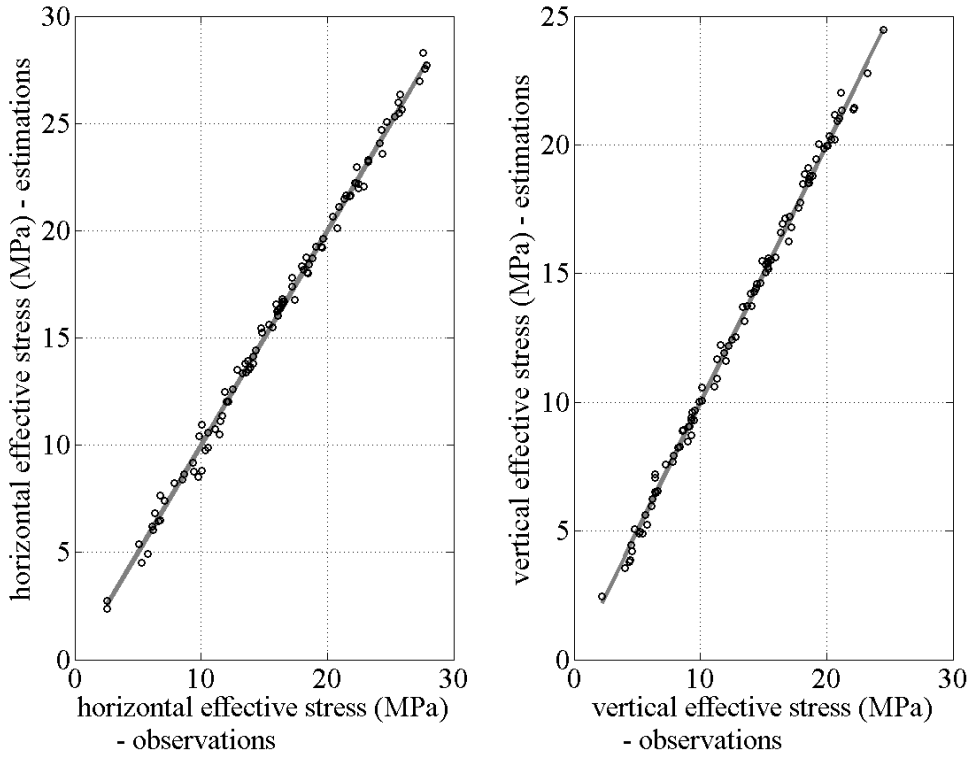

Fig. 4 - Cross validation procedure for the response surface model respectably associated with the horizontal (left figure) and the vertical (right figure) effective stress; dots represent the effective stress components estimated by the response surface.

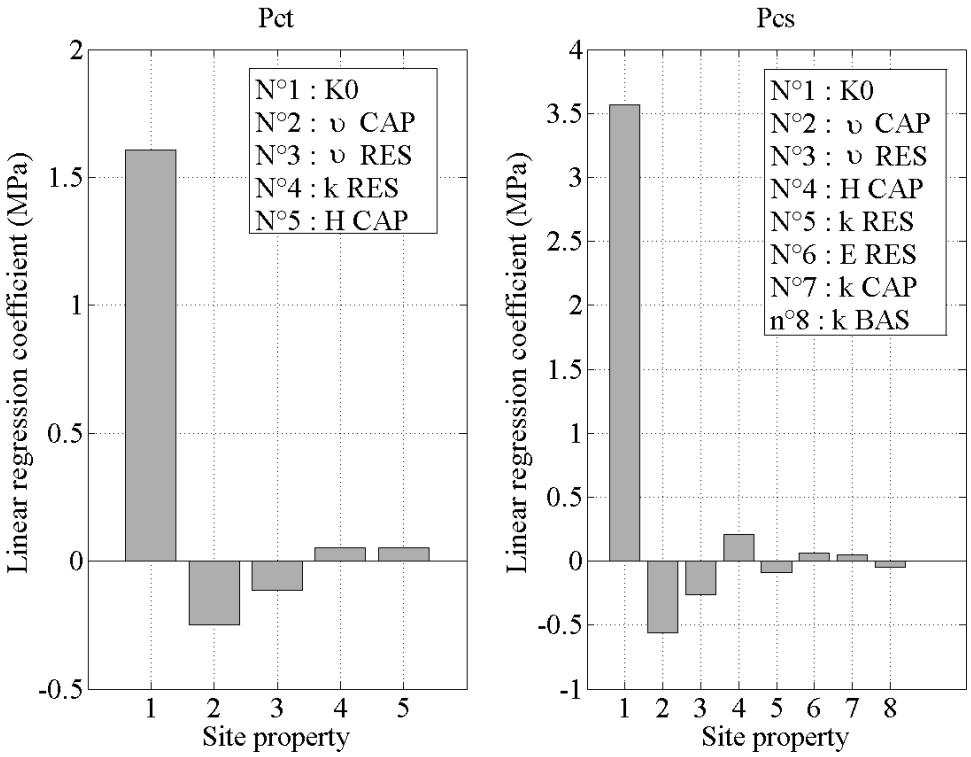
Pct
Linear regression coefficient (MPa)
Site property
N°1 : K0
N°2 : υ CAP
N°3 : υ RES
N°4 : k RES
N°5 : H CAP
Pcs
Linear regression coefficient (MPa)
Site property
N°1 : K0
N°2 : υ CAP
N°3 : υ RES
N°4 : H CAP
N°5 : k RES
N°6 : E RES
N°7 : k CAP
n°8 : k BAS

Fig. 5 - Linear regression coefficients associated with the maximal sustainable overpressure for the tensile failure mechanism (left figure) and for the shear slip failure mechanism (right figure).

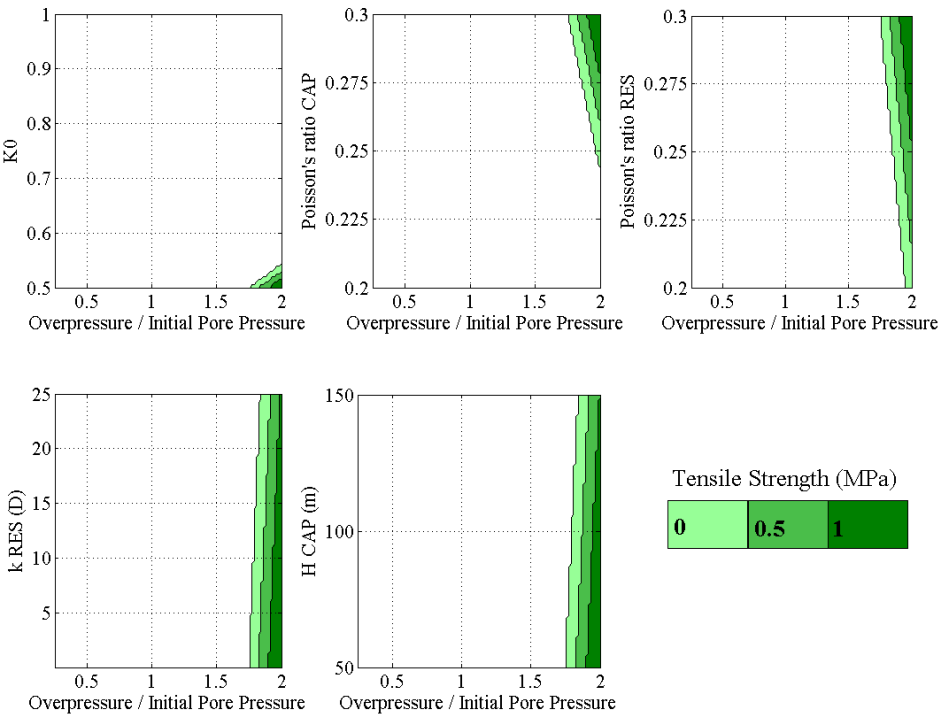

Fig. 6 - Abacus of the overpressure (in fraction of the initial pore pressure) versus the most influential site properties for the tensile fracturing criterion.

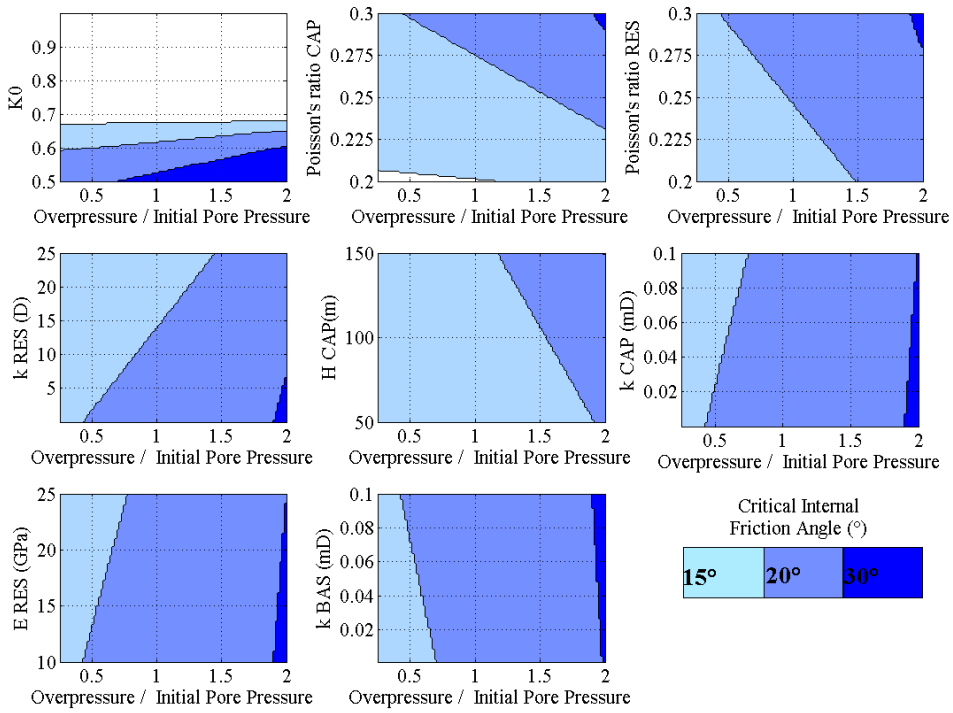

Fig. 7 - Abacus of the overpressure (in fraction of the initial pore pressure) versus site properties for the shear slip reactivation criterion considering a cohesionless pre-existing fault.

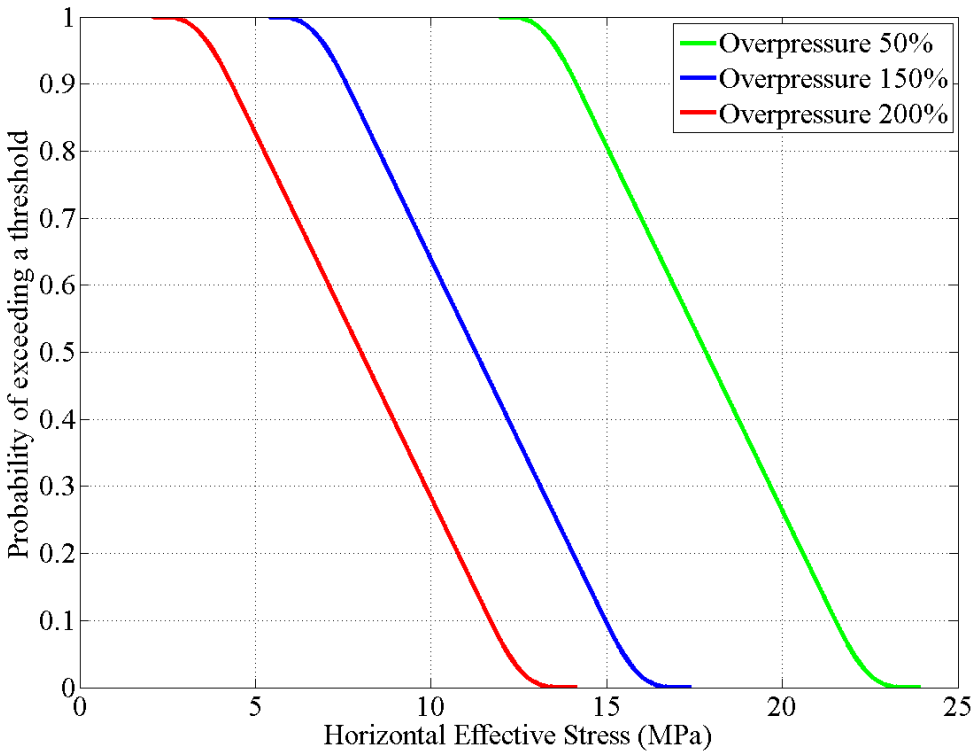

Fig. 8 - Probability of exceeding a threshold of horizontal effective stress in the Paris Basin case.

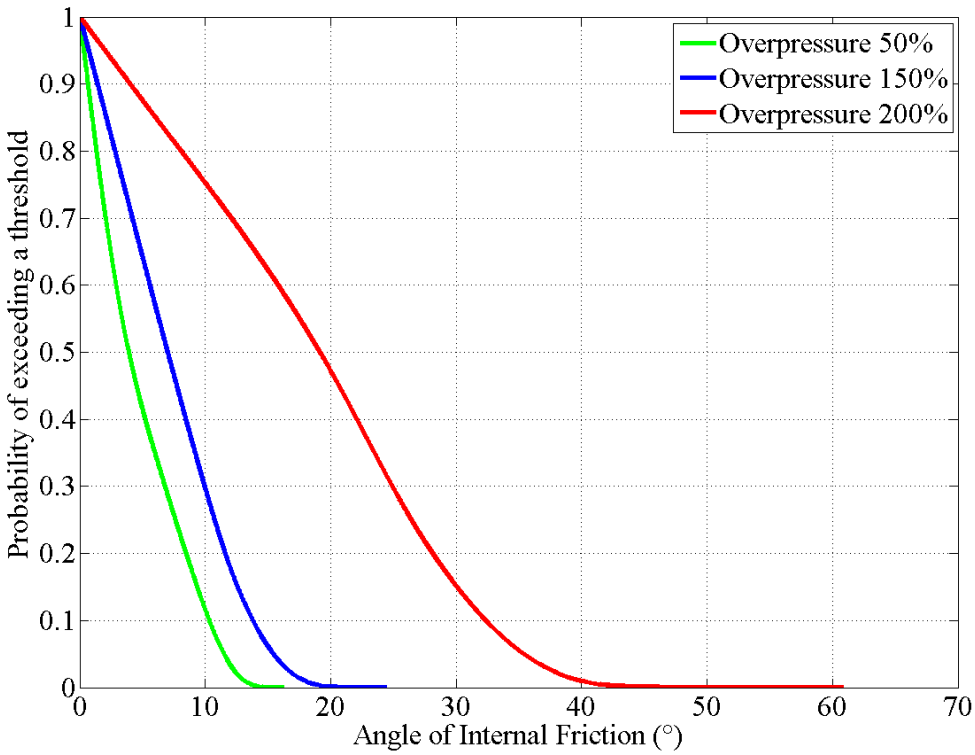

Fig. 9 - Probability of exceeding a threshold of angle of internal friction to reactivate a cohesionless pre-existing fault in the Paris Basin case.

LIST of TABLES

Table 1: Definition of the site properties for the construction of the response surface models

Input variable		Lower bound	Upper bound	Unit
Young's modulus	E_{CAP}	5	20	(GPa)
	E_{RES}	10	25	(GPa)
	E_{BAS}	25	50	(GPa)
	E_{OVE}	5	15	(GPa)
Poisson's ratio	υ_{CAP}	0.2	0.3	(-)
	υ_{RES}	0.2	0.3	(-)
	υ_{BAS}	0.2	0.3	(-)
	υ_{OVE}	0.2	0.3	(-)
Porosity	ω_{CAP}	1	5	(%)
	ω_{RES}	10	20	([%)
	ω_{BAS}	1	5	(%)
	ω_{OVE}	10	20	(%)
Intrinsic permeability	k_{CAP}	0.000001	0.1	(mD)
	k_{RES}	0.01	25.0	(D)
	k_{BAS}	0.001	0.1	(mD)
	k_{OVE}	0.01	1.0	(D)
Thickness	H_{CAP}	50	150	(m)
	H_{RES}	50	150	(m)
Initial stress state K_0		0.5	1.0	(-)
Injection Pressure P_{inj}		1.25	3.0	Fraction of the initial pore pressure

Table 2: Critical configuration of the site properties to minimize the maximal sustainable overpressure for tensile failure mechanism P_{ct} and for shear slip failure mechanism P_{cs} ("min" means minimal value and "MAX" means maximal value)

	K_0	υ_{CAP}	υ_{RES}	k_{RES}	H_{CAP}	E_{RES}	k_{CAP}	k_{BAS}
P_{ct}	*min*	**MAX**	**MAX**	*min*	*min*	Not included	Not included	Not included
P_{cs}	*min*	**MAX**	**MAX**	*min*	**MAX**	*min*	*min*	*min*

Table 3 : Assumptions for the probabilistic distributions associated with the site properties in the Paris basin case

Site property	Unit	Mathematical representation	Parameters	References
K_0	(-)	Uniform distribution	Lower bound =0.6 Upper bound =0.85	Cornet and Burlet, 1992; Vidal-Gilbert et al., 2008
υ_{CAP} υ_{RES}	(-)	Uniform distribution	Lower bound =0.2 Upper bound =0.3	Vidal-Gilbert et al., 2008
E_{RES}	(GPa)	Uniform distribution	Lower bound =20 Upper bound =25	Vidal-Gilbert et al., 2008
H_{CAP}	(m)	interval	Lower bound =50 Upper bound =100	Grataloup et al., 2008 ; Brosse et al., 2006
k_{RES}	(D)	Empirical probability distribution	Confidence interval at 95 % =[0.122 ; 9]	Permeability measurements in the Dogger layer based on Rojas et al., 1989
Log(k_{CAP})	(Log(mD))	Truncated normal	Mean =-3 Standard deviation=1 Validity domain: [-6 ; -1]	Kovscek and Wang, 2005; Brosse et al., 2006; Grataloup et al., 2008
Log(k_{BAS})	(Log(mD))	Truncated normal	Mean =-2 Standard deviation=2 Validity domain: [-3 ; -1]	Kovscek and Wang, 2005; Brosse et al., 2006; Grataloup et al., 2008